Research on the influence of particle size distribution of high-quality recycled coarse aggregates on the mechanical properties of recycled concrete

Zong, Shuai; Chang, Cheng; Rem, Peter; Gebremariam, Abraham T.; Di Maio, Francesco; Lu, Yiyan

DOI
10.1016/j.conbuildmat.2025.140253

Publication date
2025

Document Version
Final published version

Published in
Construction and Building Materials

Citation (APA)
Zong, S., Chang, C., Rem, P., Gebremariam, A. T., Di Maio, F., & Lu, Y. (2025). Research on the influence of particle size distribution of high-quality recycled coarse aggregates on the mechanical properties of recycled concrete. *Construction and Building Materials*, *465*, Article 140253. https://doi.org/10.1016/j.conbuildmat.2025.140253

Construction and Building Materials 465 (2025) 140253

Contents lists available at ScienceDirect

Construction and Building Materials

journal homepage: www.elsevier.com/locate/conbuildmat

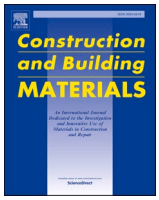

Research on the influence of particle size distribution of high-quality recycled coarse aggregates on the mechanical properties of recycled concrete

Shuai Zong [a,b], Cheng Chang [b,*], Peter Rem [b], Abraham T. Gebremariam [b], Francesco Di Maio [b], Yiyan Lu [a,*]

[a] School of Civil Engineering, Wuhan University, Wuhan 430072, China
[b] Resource & Recycling, Department of Engineering Structures, Faculty of Civil Engineering and Geosciences, Delft University of Technology, Stevinweg 1, Delft 2628 CN, the Netherlands

ARTICLE INFO

Keywords:
High-quality recycled coarse aggregates
Recycled concrete
Particle size distribution
Elementary mechanical behaviour

ABSTRACT

To alleviate the excessive extraction from natural resources and to properly manage construction waste, recycled concrete technology is globally recognized as an eco-friendly way to address these escalating challenges. This study explores the influence of three particle size distributions (PSD) (upper, median, and lower limits) and two curing conditions (normal: 19–25 °C, humidity 48–56 %; lab standard: 20 ± 2 °C, humidity ≥ 95 %) on the compressive strength, tensile splitting strength, and strength development of recycled concrete through a series of experiments. The detailed data make up the research gap in this aspect and reveal that the influence of the PSD on the compressive strength and tensile splitting strength is limited. However, a favourable curing condition benefits the mechanical properties of recycled concrete, especially in resisting tension. In terms of compressive strength, this study indicates that recycled concrete has the potential to replace natural aggregates totally and is feasible to be applied in almost all practical engineering applications, which provides a solid foundation for the future of sustainable construction.

1. Introduction

Aggregates (sand and gravel) have accounted for the largest volume of solid material extracted globally as the aggregate demand increases. The rapidly growing consumption of natural aggregates will result in environmental degradation, including river pollution, accelerated beach erosion, and the depletion of water tables [1,2]. Meanwhile, in another aspect, natural disasters, renewing, and building ageing generate enormous construction and demolition waste (C&DW). For instance, approximately 135.6 million tons of C&DW were generated annually in the US in 1990. By 2018, it reached 600.3 million tons [3]. Around 766.3 million tons (2004), 876.0 million tons (2010), and 932.7 million tons (2016) of C&DW were generated in the EU [4]. In China, the current annual output of C&DW exceeded a staggering 2000 million tons [5]. However, the majority of C&DW is still predominantly managed through piling or landfilling, inevitably causing air pollution and soil and groundwater contamination, as well as large energy consumption for transportation processes. Therefore, recycling and reusing for C&DW will protect the environment, reduce the excessive extraction from natural resources, and improve material efficiency.

For general modern buildings, concrete has become the most used construction material, with a consumption of about 0.2–0.4 m^3/m^2. Therein, structure members like beams, floor slabs, shear walls, and columns could all be recycled and reused by sorting and crushing to be recycled coarse aggregates (RCA). Fine and coarse aggregates account for approximately 70–80 % of concrete in weight, which reflects the recycling and reusing rate of waste concrete in the theoretical. RCA, using recycled aggregates partially or fully to fabricate, is increasingly utilized in practical engineering [6–8], providing an eco-friendly alternative to natural aggregates. Despite their sustainability benefits, RCA face challenges. Numerous studies have shown and indicated that recycled concrete exhibits various deficiencies in mechanical behaviour, including reduced compressive strength [9–11], tensile strength [12,13], flexure strength [14,15], and durability [16,17]. The above-mentioned results are attributed to different factors related to the quality of RCA. The hardened cement mortar attached to the RCA is a

* Corresponding authors.
E-mail addresses: C.Chang-1@tudelft.nl, chang-cheng@outlook.com (C. Chang), yylu901@163.com (Y. Lu).

https://doi.org/10.1016/j.conbuildmat.2025.140253
Received 8 November 2024; Received in revised form 14 January 2025; Accepted 29 January 2025
Available online 31 January 2025

crux. The hardened cement mortar forms three types of interfacial transition zones (ITZ) in the recycled concrete matrix that are vulnerable and negatively impact the macro-mechanical behaviour of recycled concrete [18]. The failure of recycled concrete results from the combined effects of ITZ failure and internal cracking of the aggregate. Thus, some proposals focus on improving the properties of the ITZ. Supplementary cementitious materials, chemical solutions, and carbon dioxide curing have been used to enhance the micro-structures of the recycled concrete [19–21]. Yet, these measures may cause secondary pollution in the ecological environment. To overcome the disadvantages of recycled aggregates, treatments such as enhanced crushing and screening [22], microwave heating [23], and electric pulsed power [24] have been tried to remove attached hardened cement mortar as much as possible to obtain high-quality recycled coarse aggregates (HqRCA).

An innovative technique named C2CA (concrete to concrete aggregates) has been proposed to address these issues efficiently, which also possesses the convenience and operability of the construction process are prioritized in practical engineering. As Fig. 1 shows, the production process of HqRCA from end-of-life concrete using the C2CA method [25–28], most of which are the size of 4.0–16.0 mm. The process is designed to be mobile, and thus, they can be directly installed and functioning close to demolition sites or ready-mix concrete plants, improving production efficiency and reducing heavy transport costs. Approximately 75 % of the concrete mass is occupied by aggregates, with about 40–45 % being coarse aggregates. The current crushing and recycling process classifies about 60–70 % of the crushed concrete as coarse aggregates. Therefore, it is essential to investigate how the PSD of the HqRCA influences the mechanical properties of recycled concrete when it is directly used in construction sites. For the PSD, the code *Aggregates for concrete* [29] rules the general grading requirements for coarse aggregate on the coarse aggregate size and mass percentage. However, the range between the specified upper limit and the lower limit is relatively wide, and until now, little research has focused on it. Thus, it is worth exploring the influence of different PSD on the compressive performance of concrete, particularly in recycled concrete made of recycled coarse aggregates. This study investigates the influence of three PSD (upper, median, and lower limits) and two curing conditions (normal: 19–25 °C, humidity 48–56 %; lab standard: 20 ± 2 °C, humidity ≥ 95 %) on the compressive strength, tensile splitting strength, and strength development of recycled concrete through 168 concrete cube specimens. The findings support and urge the use of recycled concrete in practical engineering applications.

2. Experiment procedures

2.1. Materials

The end-of-life concrete was sourced from a demolished juvenile detention centre at Eikenstein in Zeist, the Netherlands. It is a relatively young building which was built in 1998. Since the building was not built to accommodate the reuse of concrete components, it was selectively demolished in 2022. The end-of-life concrete was crushed with mobile crushers and later processed with C2CA technologies to separate the concrete into three recycled products: RCA, recycled fine aggregates (RFA), and cement paste-rich recycled powder (CRP), as Fig. 1 shows. Herein, only the RCA with the size of 2.0–22.4 mm are used in this study and are called high-quality recycled coarse aggregates (HqRCA). This is due to the absence of contaminants (such as bricks, ceramics, glass, etc.) and the use of impact force in ADR, which facilitates the removal of friable mortar attachments from the coarse aggregate surface.

2.1.1. Coarse aggregates

2.1.1.1. Density and water absorption. Almost all published literature demonstrates that recycled coarse aggregate (RCA) possesses lower density and significant water absorption than NCA. Similarly, Table 1 lists the indices of the physical properties of NCA and HqRCA, which involve particle density on an oven-dried basis (ρ_{rd}), particle density on a saturated and surface-dried basis (ρ_{ssd}), apparent particle density (ρ_a), and water absorption as a percentage of dry mass (*WA*). For accuracy, four samples in one group are measured by following European standard 1097–6:2013 for each item. In Table 1, the data is recorded in the format ″NCA_data (HqRCA_data)″, as well as the mean of ρ_{rd}, ρ_{ssd}, ρ_a, and *WA*, which are summarised in Fig. 2. It can be observed that the density of HqRCA is about 80–90 % of NCA, whereas the water absorption of HqRCA is around three times that of NCA.

Table 1
Physical properties of NCA and HqRCA (in bracket).

	Sample 1	Sample 2	Sample 3	Sample 4
ρ_{rd} (Mg/m^3)	2.347 (1.985)	2.350 (1.960)	2.352 (1.935)	2.356 (1.952)
ρ_{ssd} (Mg/m^3)	2.399 (2.090)	2.405 (2.090)	2.406 (2.064)	2.410 (2.059)
ρ_a (Mg/m^3)	2.476 (2.256)	2.486 (2.252)	2.486 (2.222)	2.490 (2.223)
WA (%)	2.223 (6.730)	2.331 (6.612)	2.276 (6.692)	2.292 (6.973)

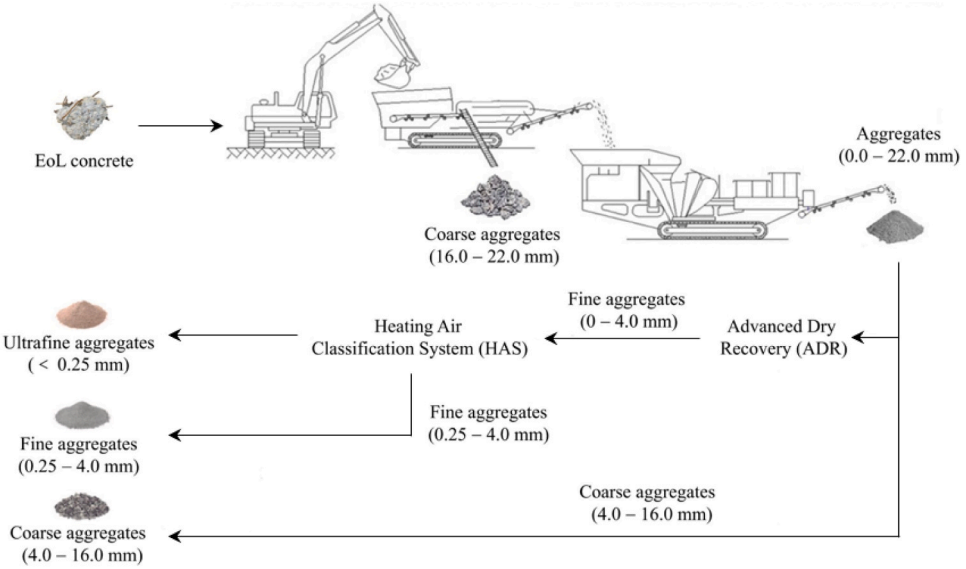

Fig. 1. The process of converting end-of-life concrete into recycled aggregates.

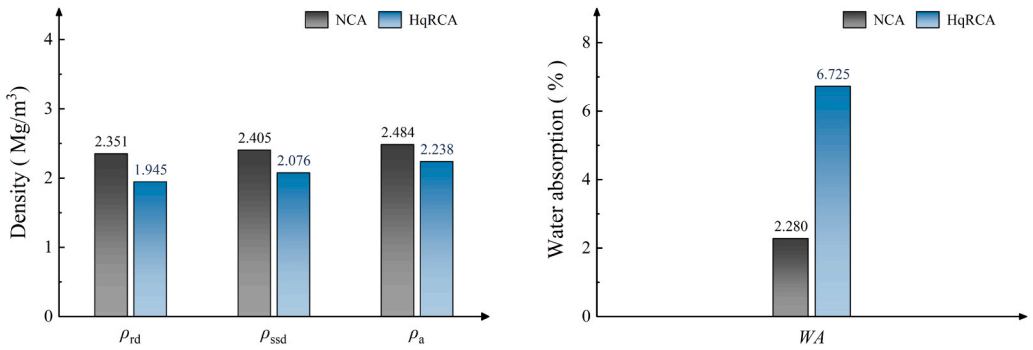

Fig. 2. Averages of density and water absorption.

2.1.1.2. Los Angeles coefficient and aggregates crushing value. The Los Angeles coefficient (*LA*) and aggregates crushing value (*ACV*), according to BS EN 1097–2:2020 and BS 812–110:1990, are used in this study to characterize the physical and mechanical properties of the coarse aggregates in a comparative way. In the Los Angeles test, the coarse aggregates are subjected to the combinational environment of grinding and crashing, which are applied to evaluate the resistance to fragmentation of the coarse aggregates. It is meant to assess the potential particle size change of ready-mixed concrete made from HqRCA during transportation. *ACV* is suitable for measuring the crushing resistance of the coarse aggregates under increasing load. Three samples in one group are tested; the *LA* and *ACV* are depicted in Fig. 3, where the larger the value, the weaker the resistance of coarse aggregate to wearing and crushing.

2.1.2. Fine aggregates and cement

The river sand, GEBROKEN ZAND 0–4 mm, is used as fine aggregates. The details of fine aggregates are listed in Table 2, and the corresponding curve of the particle size distribution is also drawn in Fig. 4. HOOGOVEN CEMENT CEM III 42.5, a kind of blast furnace cement, is selected as the cementitious material, and its components are listed in Table 3. The application of composite cement not only reutilizes industrial waste but also can improve concrete durability. Replacing a portion of the rapidly hydrating Ordinary Portland Cement (OPC) with latent hydraulic, slower-reacting ground granulated blast furnace slag (GGBFS) reduces the heat production rate and the total heat of hydration, which is particularly beneficial for casting mass concrete, as it helps to avoid thermal shrinkage cracking [30,31].

Table 2
The characteristics of fine aggregates.

	Particle density (Mg/m^3)	Water absorption (%)	Moisture content (%)
GEBROKEN ZAND	2.625 Fineness modulus 3.09	3.82 Clay content (%) 0.7	1.4 Shell content (%) < 0.1

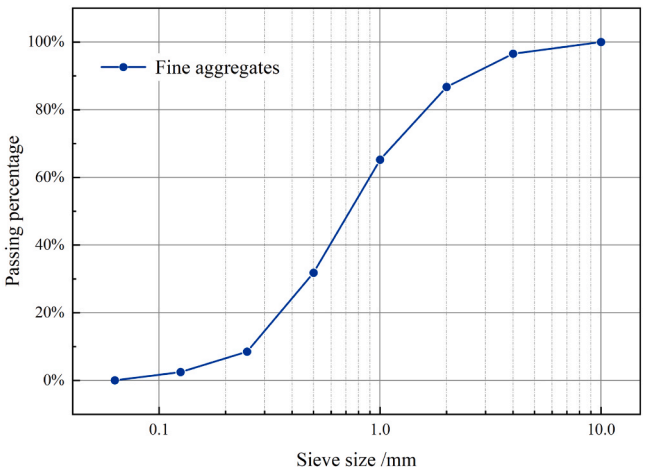

Fig. 4. Particle size distributions of fine aggregates tested.

2.2. Particle size distribution (PSD)

The cumulative percentage retained is used to exhibit the general grading requirements of coarse aggregates, including the upper limit, median level, and lower limit, which are based on European standard 12620:2013, as depicted in Fig. 5. Herein, the coarse aggregate size interval is further subdivided according to the linear interpolation marked with an asterisk superscript. The shadow area fills the whole ruled range, and the sector diagrams are used to present the proportions of each size of coarse aggregates. Moreover, in the experiment, the

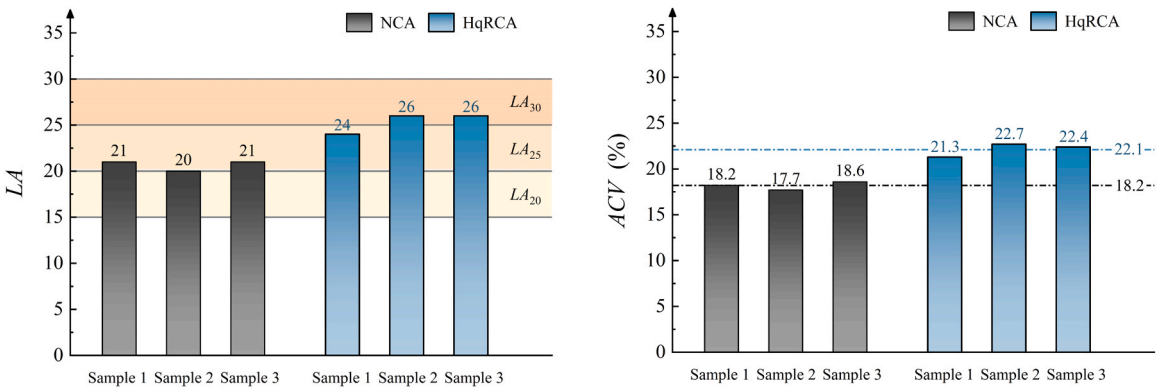

Fig. 3. Los Angeles coefficient and aggregates crushing value.

Table 3
The components of the cement.

				Pozzolana		Flyash		
Type	Clinker K	GGBF S	Silica fume D	Natural P	Industrial Q	Siliceous V	Calcareous W	Other
III 42.5	35–64 %	36–65 %	-	-	-	-	-	0–5 %

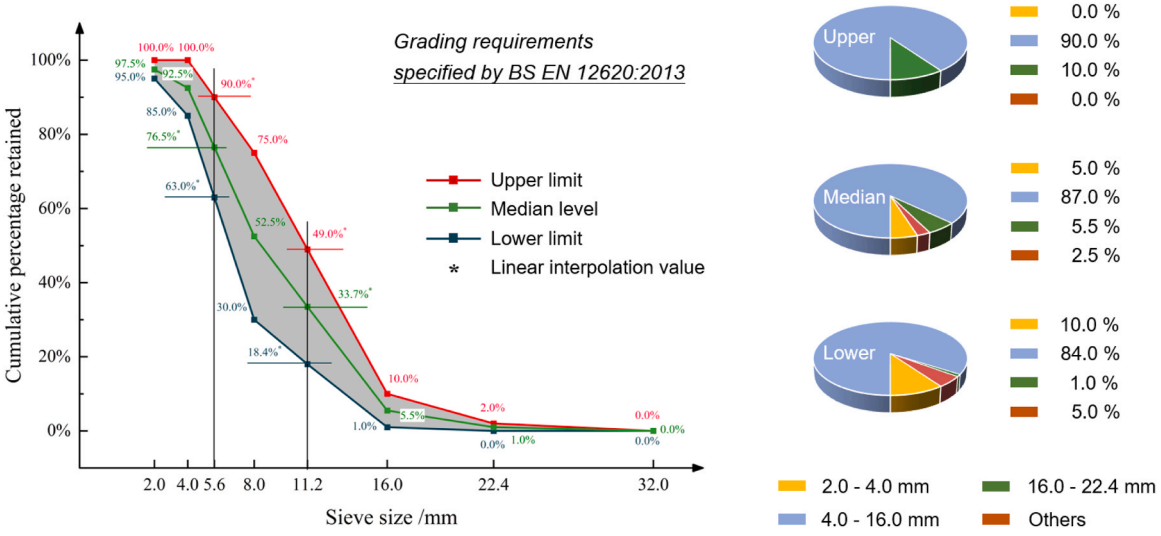

Fig. 5. General grading requirements of coarse aggregates.

aggregates smaller than 2.0 mm and those bigger than 22.4 mm are removed to focus on the size range of the coarse aggregate within 2.0–22.4 mm, as shown in Fig. 6. Meanwhile, to ensure the accuracy of the amount of coarse aggregate used in the experiments, both HqRCA and NCA are sieved into specific size ranges, as shown in Fig. 7.

2.3. Concrete proportion

All concrete specimens were prepared using the same mix design, as presented in Table 4. The concrete recipe was calculated according to the "mass method", with the mass of the mixture per unit volume (1 m^3) set at 2400 kg. For the recycled concrete, NCA was entirely replaced with HqRCA of the same mass. To fully utilize the mechanical properties of HqRCA, the 28-day compressive strength of the recycled concrete was targeted at 60 MPa. Additionally, the water-to-cement ratio is a critical factor influencing the strength of concrete. Many studies recommend pre-wetting recycled coarse aggregates to a saturated surface-dry condition during the preparation of recycled concrete, aiming to prevent the recycled aggregates from affecting the actual water-to-cement ratio of the mixture during mixing. However, this operation remains controversial in practical applications, as it is often influenced by the casting volume and could lead to segregation, significantly impacting the mechanical properties of recycled concrete [32–35]. Therefore, during the calculation process, the amount of mixing water accounted for the moisture content of coarse and fine aggregates, and the total mixing water content was kept constant. The moisture content of the coarse aggregates used in this experiment was highly similar, so the amount of mixing water was not calculated separately. The superplasticizer,

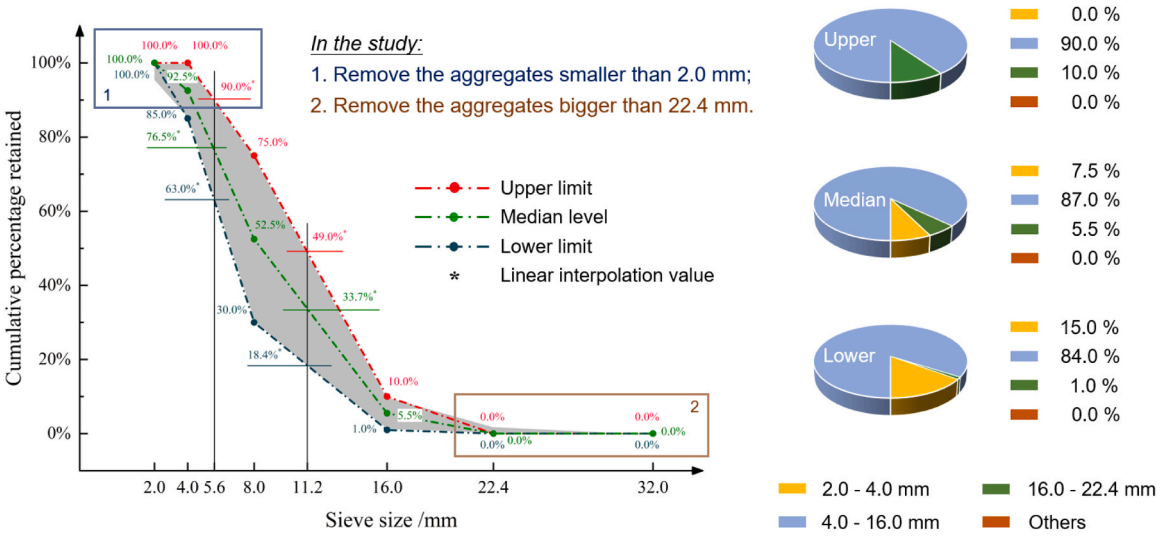

Fig. 6. The PSD of coarse aggregates adopted in the experiment.

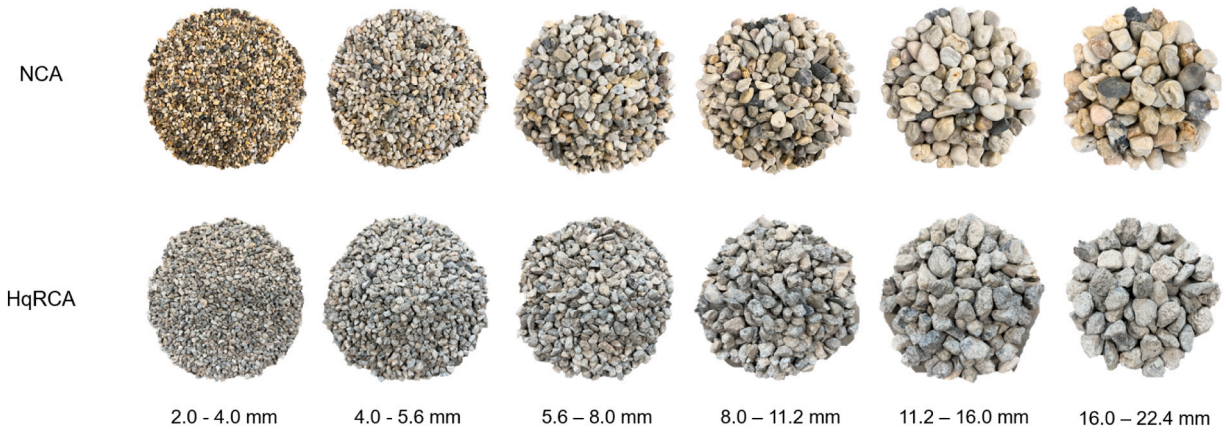

Fig. 7. The sieved coarse aggregates.

Table 4
The proportion for all the concrete specimens (per 1 m^3).

Coarse aggregates	Sand	Water	Cement	Superplasticizer
1017.5 kg	832.5 kg	151.5 kg	382 kg	1.33 kg (0.35 %)

SIKA-VC 1550 con. 30 % was used at 0.35 % of the cement mass to improve the mixture fluidity.

Common experimental design methods include full factorial experimental design and orthogonal experimental design. Full factorial design allows for a comprehensive consideration of the effects of various factors and their interactions on the results; however, it requires a large number of specimens. By contrast, orthogonal experimental design selects a small number of representative experimental points for significance analysis, but the limited sample size may not adequately reflect the influence patterns of individual factors. This study primarily focused on the influence of various parameters on the mechanical behaviour of recycled concrete and thus employed a full factorial experimental design for arranging recycled concrete specimens. For the normal concrete specimens acting the role as the reference, not all possible factor-level combinations were considered; instead, a subset of factor combinations was selected for testing. Since the compressive strength of concrete at 28 days is relatively important, this study chose to use the full factorial design for settling the normal concrete specimens for testing their 28 days compressive strength, while other normal concrete specimens were designed based on the median level of coarse aggregate gradation curves, with the strengths used as references. Based on the methods mentioned above, as Fig. 8 shows, a total of 168 standard concrete cube specimens with side lengths of 150 mm are cast. Herein, 108 recycled concrete specimens were prepared by using HqRCA to investigate the influence of the PSD, curing conditions and concrete age on the compressive strength and splitting tensile strength of recycled concrete; meanwhile, 60 normal concrete specimens were, as references, prepared by using NCA.

2.4. Curing condition and concrete age

Two types of curing conditions, normal curing and lab standard curing, are considered because the actual construction conditions are always different from those in the laboratory. For the normal curing condition, without extra special measures, the temperature is 19–25 °C, and the humidity is 48–56 % is used. For the standard laboratory condition, the temperature and humidity are 20 ± 2 °C and greater than 95 %, respectively. The concrete ages include 14, 28, and 91 days to observe the development trends of concrete strengths.

2.5. Testing process

All concrete specimens are tested in the electric-servo testing machine, as shown in Fig. 9, and the processes for testing compressive strength and tensile splitting strength of concrete specimens follow the European codes 12390-3: 2019 [36] and 12390-6: 2023 [37]. For testing compressive strength, a constant rate of loading of 0.7 MPa/s is selected; for testing tensile splitting strength, a constant rate of stress of 0.05 MPa/s is set. After the application of the initial load, which does not exceed approximately 20 % of the failure load, the load to the

Test / Time		14 days				28 days				91 days			
Specimens		Compression test		Tensile splitting test		Compression test		Tensile splitting test		Compression test		Tensile splitting test	
Recycled concrete	Upper	3	3	3	3	3	3	3	3	3	3	3	3
	Median	3	3	3	3	3	3	3	3	3	3	3	3
	Lower	3	3	3	3	3	3	3	3	3	3	3	3
Normal concrete	Upper	-	-	-	-	3	3	3	3	-	-	-	-
	Median	3	3	3	3	3	3	3	3	3	3	3	3
	Lower	-	-	-	-	3	3	3	3	-	-	-	-

Notes: Normal curing; Lab standard curing

Total: 168
Valid data: 166

Fig. 8. Samples overview.

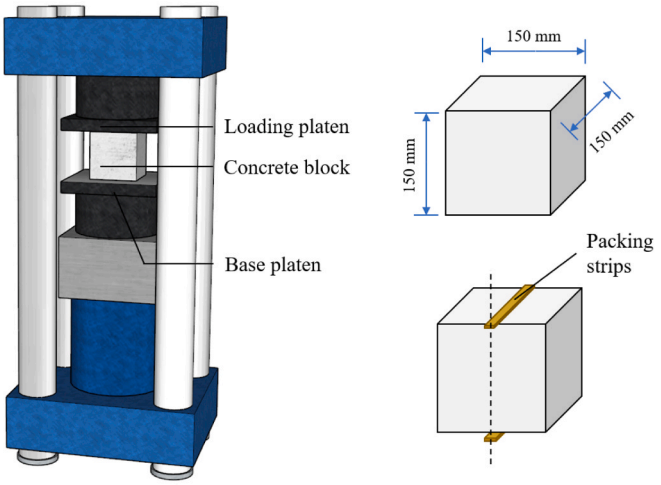

Fig. 9. Testing apparatus and concrete specimens.

specimen without shock increases continuously. Meanwhile, a pair of one-time packing strips are used, which are made of hardboard of 15 mm dimensions width and 3 mm thickness and a length longer than that of the tested specimen.

3. Experiment results and discussions

3.1. Compressive strength (f_{cu})

As a crucial index for concrete strength, the 28 days compressive strengths ($f_{cu,28d}$) of recycled concrete and normal concrete specimens are shown in Fig. 10. Different coloured columns within the same colour scheme represent different specimens. The mean and error bars for each group of three samples are added as well. In terms of the $f_{cu,28d}$ of concrete specimens, it is feasible to use HqRCA to fully replace NCA in preparing recycled concrete to gain a favourable compressive strength of concrete. Under the normal curing condition and the lab standard curing condition, the average compressive strength of the recycled concrete reached 64.40 MPa and 64.95 MPa, respectively. Regarding the concrete strengths, theoretically, it could meet the requirements of most construction applications; however, the experimental result contrasts with the held belief that substituting NCA with RCA would significantly discount the compressive strength of concrete. Similar findings have been reported in the literature [38]. Additionally, the $f_{cu,28d}$ of concrete specimens appeared to exhibit an increasing trend as the aggregate gradation shifted to the lower limit. As the PSD shifted toward the lower limit, compared to specimens with upper-limit gradation, the average $f_{cu,28d}$ of recycled concrete specimens under the lab standard curing condition increased by 2.6 % and 4.8 %; under the normal curing condition, the average $f_{cu,28d}$ of normal concrete specimens increased by 5.0 % and 8.7 %, respectively, while under the lab standard curing condition, the increases reached 8.6 % and 10.4 %.

Several factors contribute to these observations:

- Aggregates and gradations

Firstly, the compressive crushing performance of HqRCA is not significantly inferior to that of NCA, as exhibited in the *ACV*. Second, the gradation of the coarse aggregates followed a continuous grading composed of multi-particle size groups, resulting in a relatively dense concrete skeleton [39]. Moreover, the experimental results indicate that the compressive strength of concrete specimens appeared to increase as the PSD curve shifted from the upper limit to the lower limit. The same findings also occurred in the normal concrete specimens. This may be because under the same mass condition, as the PSD of coarse aggregates changes from upper towards lower, the proportion of coarse aggregates with small size increases, which may improve the compactness of concrete matrix and alleviate the internal bleeding that possibly occurs on the large granular aggregates due to gravity-induced migration because of the larger the aggregate particle size, the more pronounced the tendency for water film accumulation on the aggregate surface in which the interfacial transition zone is prone to form micro-cracks [40]. Also, in the fracture process of concrete, cracks generally tend to grow along the aggregate boundary, namely interfacial transition zones, as it is a weak part of concrete. Therefore, the cracks easily propagate along a large aggregate because of consecutive areas of interfacial transition zones. The rapid growth of cracks tends to break through the mortar ahead. However, such is alleviated in concrete made with small aggregates, as interfacial transition zones are discontinuous, and mortar restrains crack growth. Thus, cracks stop advancing unless higher loadings are applied, which leads to a slower cracking process and a higher compressive strength [41].

- Effective water-to-cement ratio

Due to the mixing water content in the concrete recipe (Table 4) remained constant, the higher water absorption characteristics of HqRCA, when replaced NCA by the same mass, reduced the effective water-to-cement ratio of the concrete during the hardening process, as shown in Fig. 11. This could enhance the compressive strength of the recycled concrete. Furthermore, if the overall particle size of the HqRCA

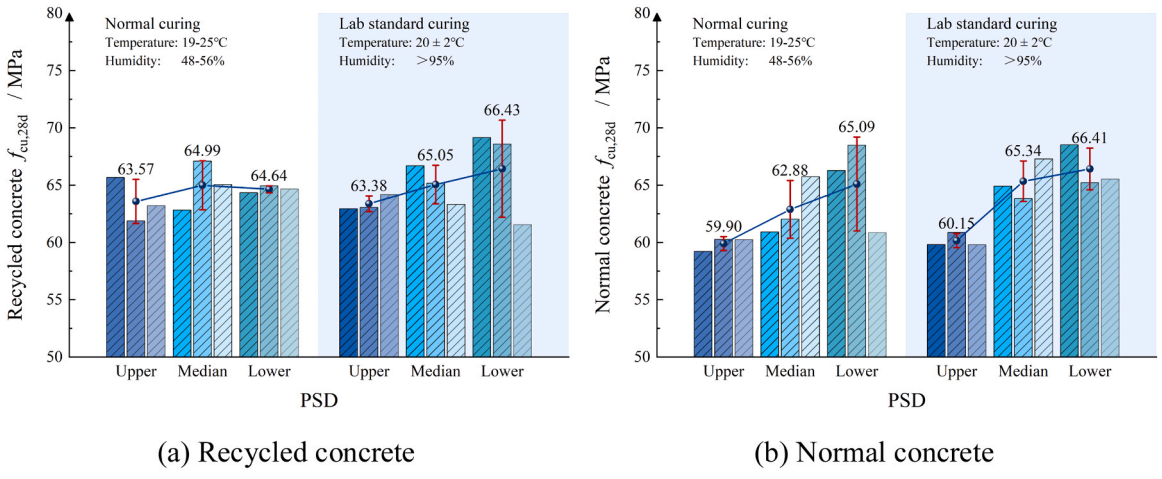

Fig. 10. The $f_{cu,28d}$ of recycled concrete and normal concrete.

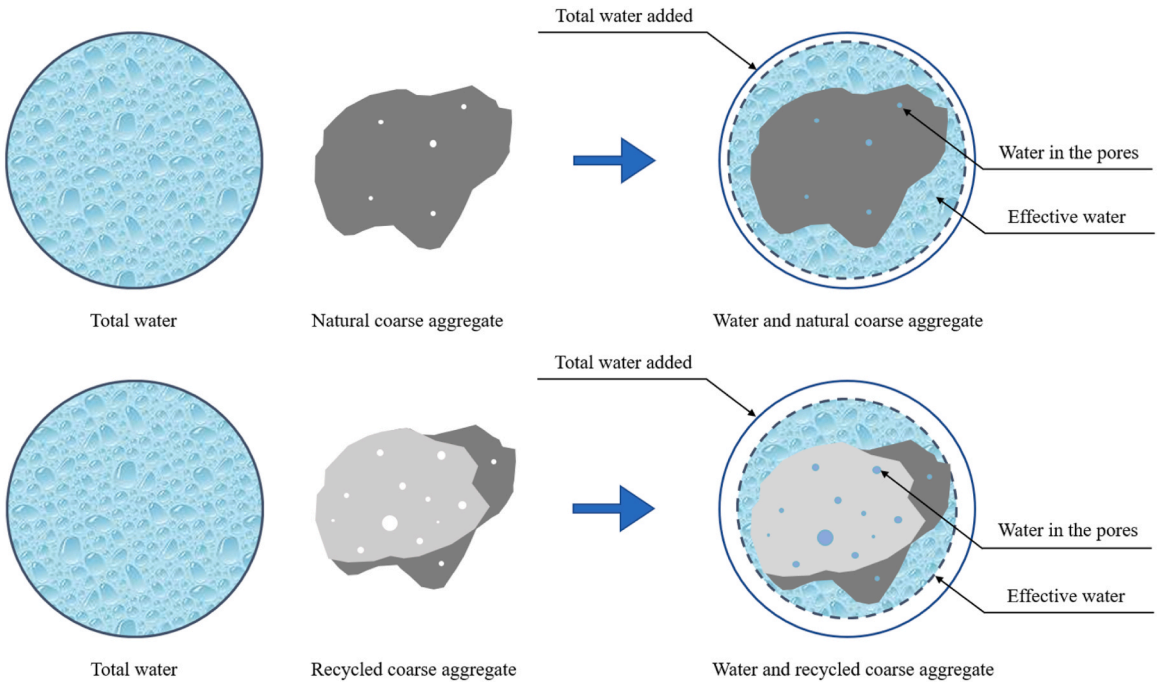

Fig. 11. Effective water on natural concrete and recycled concrete.

is relatively small—i.e., the PSD curve shifts toward the lower limit—the increased surface area of the coarse aggregates may exacerbate this effect [42].

To validate this hypothesis, a simple model is established to roughly estimate the surface area of coarse aggregates based on the following assumptions:

1) The coarse aggregate is treated as a rigid pellet;
2) The influence of the contact area among the pellets on the surface area is ignored;
3) The accumulation conditions of the aggregates are not considered;
4) The density and mass of each rigid pellet are uniform;
5) Take no account of the size effect for concrete block.

Complying with assumptions above, the mass of the coarse aggregates in each particle size interval can be expressed in the following formula:

$$\boldsymbol{m} = (m_1, \quad m_2, \quad \dots, \quad m_6)^{\mathrm{T}} \tag{1}$$

$$\boldsymbol{p} = (p_1, \quad p_2, \quad \dots, \quad p_6)^{\mathrm{T}} \tag{2}$$

$$M = \sum_{\mathrm{i}=1}^{6} m_{\mathrm{i}} \tag{3}$$

$$\boldsymbol{m} = M \cdot \boldsymbol{p} \tag{4}$$

Where $\boldsymbol{m}$ is the mass matrix, herein, m_1 represents the mass of the coarse aggregates within 2.0 mm to 4.0 mm; m_2 represents that of the coarse aggregates within 4.0 mm to 5.6 mm; and so forth, m_6 is the mass of the coarse aggregates within 16.0 mm to 22.4 mm. M is the total mass of the coarse aggregates, and $\boldsymbol{p}$ is the proportion matrix that describes the ratio of the mass of the coarse aggregates in a certain particle size interval to that of total coarse aggregates. r_{i} is the radius of the rigid pellet, which is adopted by the mean of the maximum and minimum values of each particle size interval. Here, the count of rigid pellets within a specified particle size interval (n_{i}) and the surface area of total coarse aggregates (S) can be derived.

$$n_i = \frac{3}{4} \cdot \frac{m_{\mathrm{i}}}{\rho \, \pi r_{\mathrm{i}}^3} \tag{5}$$

$$\boldsymbol{n} = (n_1, \quad n_2, \quad \dots, \quad n_6)^{\mathrm{T}} \tag{6}$$

$$S = 4\pi \, \boldsymbol{r}^{\mathrm{T}} \boldsymbol{r} \cdot (1, \quad 1, \quad \dots, \quad 1) \boldsymbol{n} \tag{7}$$

Where ρ is the density of the coarse aggregates, and $\boldsymbol{r}$ is the radius matrix. According to Eqs.(1)–(7), for the same aggregates, the surface area of the coarse aggregates with the lower PSD is approximately 24.1 % and 63.5 % larger than that of the coarse aggregates with the median PSD and upper PSD, respectively. If r_{i} approaches the minimum of the interval, the increment will further grow to 27.3 % and 75.2 %. S is the function of the total mass of the coarse aggregates M, the distribution proportion p, and the density of the coarse aggregates ρ, namely $S = S(M, p, \rho)$, meaning the casting volume and particle density influence S value. This indicates that a small-scale casting volume could diminish the difference and that when HqRCA is used to replace NCA with the same mass, the lower density of HqRCA will increase the volumetric fraction of coarse aggregates and elevate concrete strength [43]. Also, the rougher surfaces of HqRCA may enhance the bond strength between the cement mortar and the aggregate, and under compressive loads, internal defects gradually close through frictional sliding, resulting in the densification of the concrete specimen during the initial loading phase. Within a certain range, the size of the initial defects can affect crack propagation, and when the initial defect size is small, this effect may be negligible [44,45].

- Curing conditions and strength development

Figs. 12 and 13 illustrate the 14 days compressive strength ($f_{\mathrm{cu,14d}}$) and 91 days compressive strength ($f_{\mathrm{cu,91d}}$) of recycled concrete and normal concrete. Additionally, Figs. 14 and 15 summarise the compressive strengths of all concrete specimens at different ages. The experimental results indicate that curing conditions influence the strength development of both recycled and normal concrete over time. For example, the average of the $f_{\mathrm{cu,91d}}$ of recycled concrete specimens under the lab standard curing condition is 6.51 % higher than that under

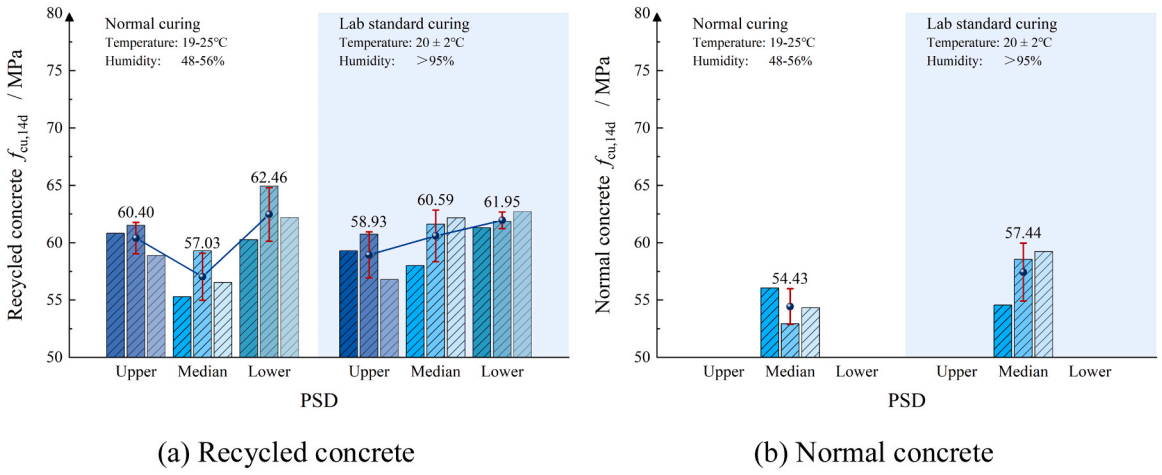

Fig. 12. The $f_{cu,14d}$ of recycled concrete and normal concrete.

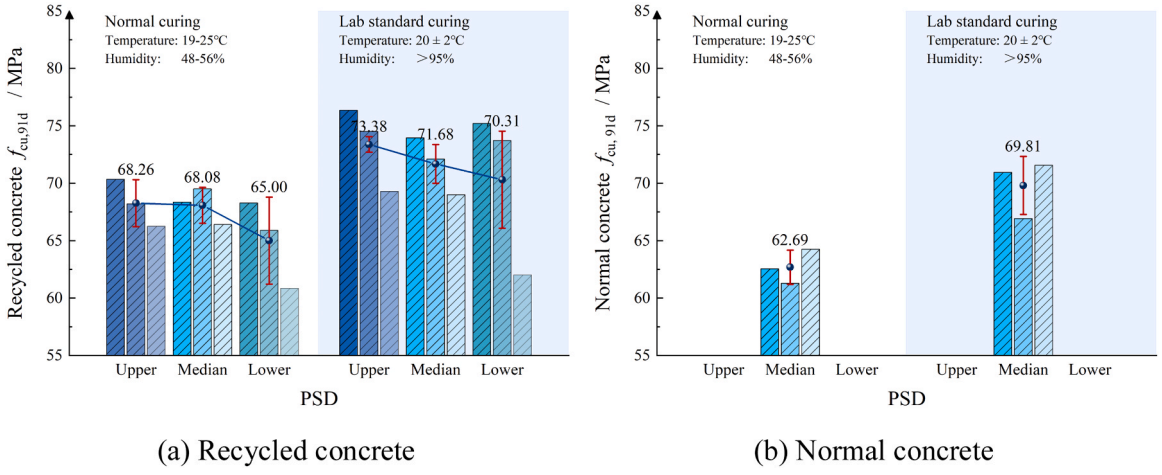

Fig. 13. The $f_{cu,91d}$ of recycled concrete and normal concrete.

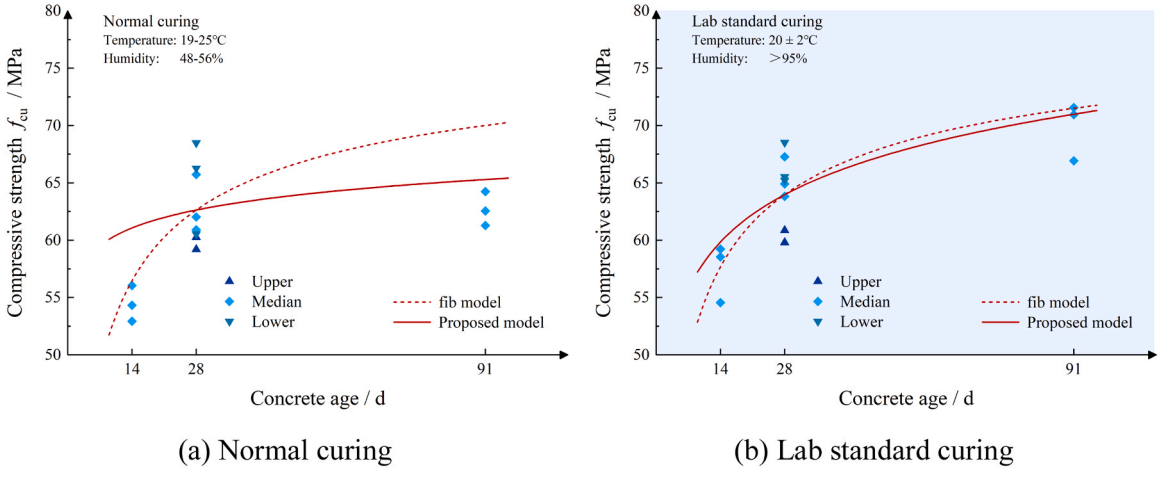

Fig. 14. The f_{cu} of normal concrete with different concrete ages.

the normal curing condition. This phenomenon arises from the obvious differences in humidity between the two curing environments. It is because curing refers to the combination of conditions promoting cement hydration. If the concrete is at a fixed water-to-cement ratio, the porosity of the hydrated cement paste depends on the degree of cement hydration. As more cement particles participate in the hydration reaction, the porosity of the concrete decreases, promoting an increase in concrete strength [46]. However, when hydration products encapsulate un-hydrated cement particles, the hydration reaction slows significantly, as sufficient hydration can only occur under saturated

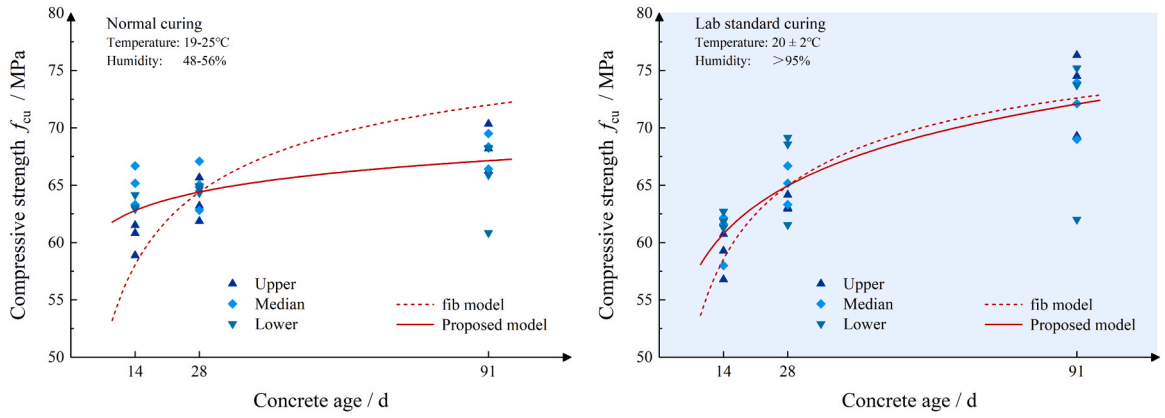

Fig. 15. The f_{cu} of recycled concrete with different concrete ages.

conditions. Under normal curing conditions, water evaporates through capillary pores, thereby impeding the hydration process, which causes slower or even stagnant strength development in the concrete. Thus, humidity is a critical factor that affects water diffusion and the hydration process, and the long-term compressive strengths of the concrete specimens under normal curing conditions exhibited limited increases.

Eurocode 2: Design of concrete structures [47] and Fib Model Code for Concrete Structures 2010 [48] provide a reference for the related compressive strength $f_{cm}(t)$ at various ages for a mean temperature of 20 °C and in the lab standard curing condition, as follows:

$$f_{cm}(t) = \beta_{cc}(t)\cdot f_{cm} \tag{8}$$

$$\beta_{cc}(t) = e^{\hat{}}\left\{s\cdot\left[1-\left(\frac{28}{t}\right)^{0.5}\right]\right\} \tag{9}$$

Where f_{cm} is the mean compressive strength in MPa at the age of 28 days, $\beta_{cc}(t)$ is a function to describe the development with time, and s is a coefficient that depends on the strength class of cement. As Fig. 15 shows, although the fib model could seemingly be applied to describe the strength development of recycled concrete, there are deviations in which the fib model estimates the compressive strength of recycled concrete specimens in normal curing conditions. Thus, a refined model should be proposed.

$$f_{cm}(t) = k\cdot f_{cm}\frac{\ln(t)}{\ln(28)} + f' \tag{10}$$

$$f' = (1-k)f_{cm} \tag{11}$$

Where k is the coefficient of strength development, and f' is the early-stage strength. Herein, the k value reflects the trend of strength development. In the study, k equals 0.12 for recycled concrete specimens under the normal curing condition and 0.31 for those in the lab standard curing condition, which means a good curing condition is beneficial to the strength development of recycled concrete. The effect of the refined model on forecasting the compressive strengths of recycled concrete specimens at different ages is displayed in Fig. 15.

3.2. Tensile splitting strength (f_{sp})

Tensile splitting strength (f_{sp}) is used to evaluate the resistance of concrete to tension and crack, which also relates to concrete durability and bond strength with steel reinforcements. The tensile splitting strengths of the specimens at the ages of 14 days, 28 days, and 91 days ($f_{sp,14d}$, $f_{sp,28d}$, and $f_{sp,28d}$) are shown in Figs. 16–18. Overall, the various PSD do not show a clear tendency on the f_{sp} of the concrete specimens tested. This may be because the changed PSD in this study does not radically affect the complex failure mechanisms of concrete under tensile splitting loads. Unlike uniaxial compression, during the tensile splitting test, the concrete within the central area of the plane between the loading points (packing strips) is in a biaxial tensile-compressive stress state. The deducted strength of the concrete under this stress distribution leads to the initiation and propagation of damage-induced

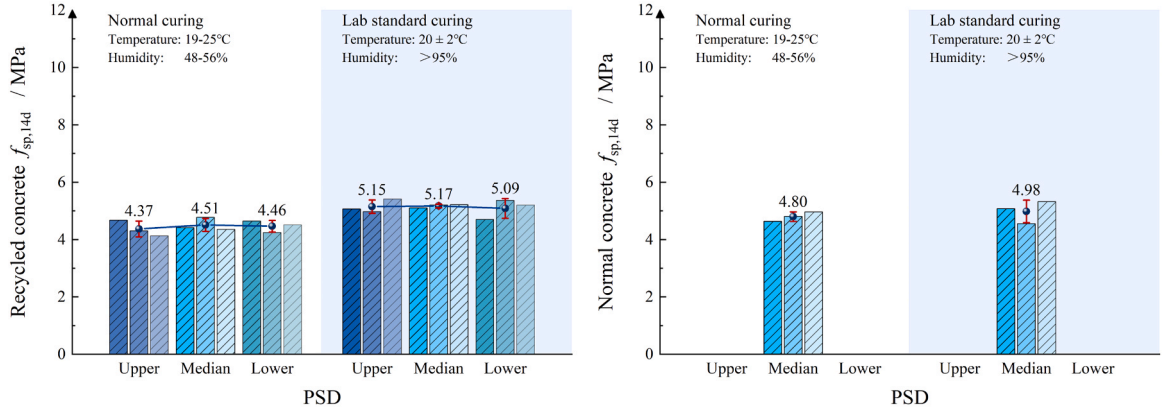

Fig. 16. The $f_{sp,14d}$ of recycled concrete and normal concrete.

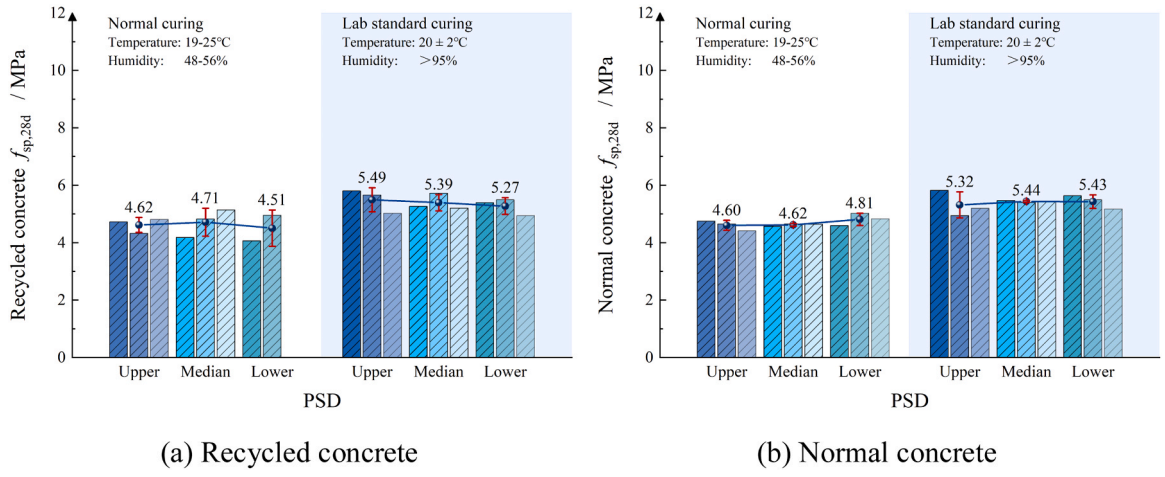

Fig. 17. The $f_{sp,28d}$ of recycled concrete and normal concrete.

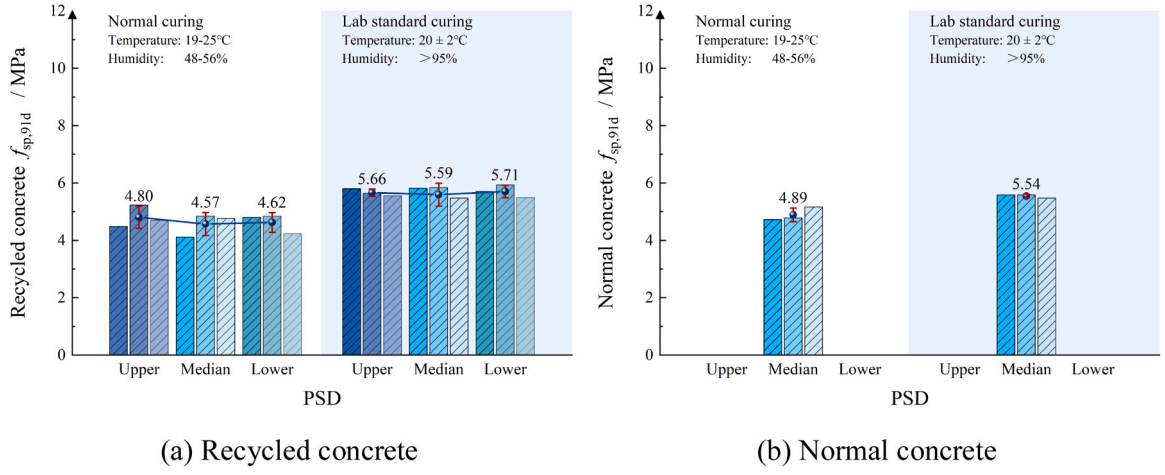

Fig. 18. The $f_{sp,91d}$ of recycled concrete and normal concrete.

cracks in weaker regions [49]. Although the ITZ and mortar are generally deemed weaker concrete regions, as crack propagation rapidly develops, cracks may penetrate the aggregates and cause failure along the concrete section. Given the relatively high strength of aggregates, this procedure potentially causes the fluctuation of f_{sp} of the concrete [50]. It also indirectly indicates that the bond strength between the cementitious matrix and the aggregates is relatively reliable; however, this phenomenon also possesses a certain degree of randomness. By contrast, the lab standard curing condition is beneficial to the f_{sp} of the specimens. The mean f_{sp} under the lab standard curing condition for the recycled

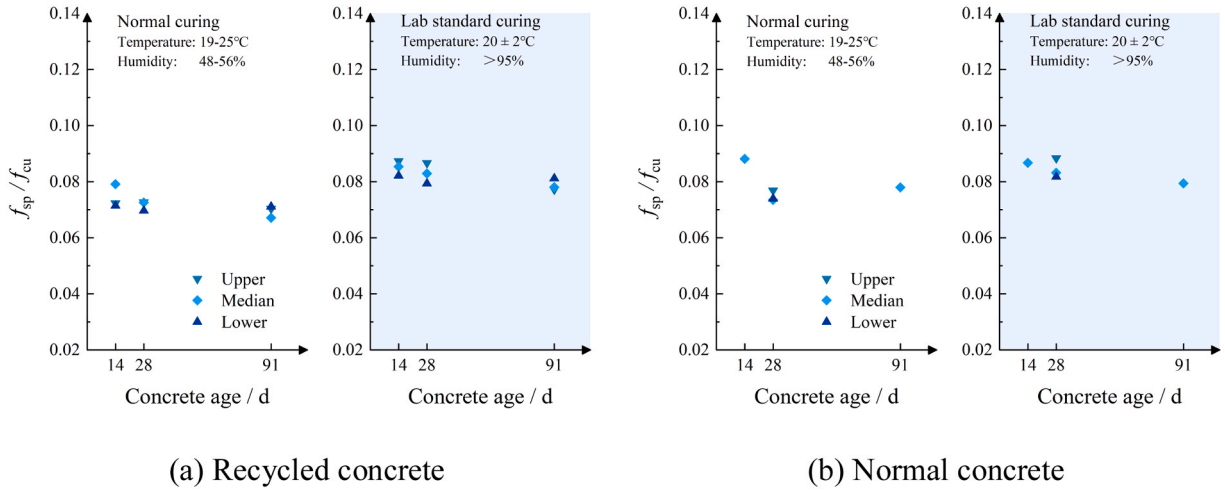

Fig. 19. The mean f_{sp} / f_{cu} of the concrete specimens.

concrete specimens is 13.40 %, 14.39 %, and 17.49 % higher than those under the normal curing condition at the concrete ages of 14 days, 28 days, and 91 days, respectively. As mentioned above, favourable curing conditions benefit the hydration reaction, enhancing the compactness of the concrete matrix and thereby improving the f_{sp} of the concrete specimens.

The ratio of f_{sp} to f_{cu} of the concrete (f_{sp}/f_{cu}) is used to reflect the brittleness of the concrete. The smaller the f_{sp}/f_{cu}, the more obvious the brittleness of concrete. As shown in Fig. 19, the f_{sp}/f_{cu} for the recycled concrete specimens is between 1/13 and 1/15 when under normal curing; under the same condition, the f_{sp}/f_{cu} of the recycled concrete specimens is slightly lower than that of the corresponding normal concrete specimens. For instance, the mean f_{sp}/f_{cu} of the recycled concrete specimens under normal curing at 14 days is only 87.0 % of that of normal concrete with the same curing condition, but it can reach 97.9 % when the specimens are under the lab standard curing condition. The results, combined with tensile splitting strength, indicate that if recycled concrete is used in practical engineering, the tension in recycled concrete members should be avoided as much as possible, and favourable curing conditions for recycled concrete members should be applied. Besides, the f_{sp}/f_{cu} gradually decreases with the increasing concrete age, which means the development in compressive strength is faster than that in tensile splitting strength.

Fig. 20 displays the failure surface characteristics of a part of the concrete specimens with different PSD after the finished tensile splitting tests. Although the coarse aggregates of the specimens have different PSD, the cross sections of their matrix are still compact, showing a multi-particle size and continuous skeleton of proportioned coarse aggregate. Compared to the recycled concrete specimens, the boundary profile and failure sections of the coarse aggregates in the normal concrete specimens are clearer and flatter. It should be noticed that numerous failure sections of the recycled coarse aggregate are distributed on both sides of the concrete section distinctly and symmetrically. Thus, it could be further concluded that many concrete cracks developed in the concrete matrix and penetrated through the coarse aggregate during the failure process of the specimens. Simultaneously, although the debonding failure mode between the hardened cement mortar attached to the HqRCA and the new cementitious matrix can also be observed according to the failure surfaces, compared to the fracture characteristics of normal concrete under tensile splitting loads, recycled concrete specimens also exhibited fracture planes with more coarse aggregate particles intersecting the fracture surface, rather than predominantly debonding failure modes. This suggests that the bond behaviour between HqRCA and the new cementitious matrix is reliable.

3.3. Standard deviation of compressive strength

The standard deviation for concrete is a method to assess the reliability of compressive results of a concrete batch. It serves as a key indicator for controlling variability in the test results of the same batch. The characteristic strength of concrete is defined as that level of strength below which a specified proportion of all valid data is expected to fail. Unless otherwise stated, this proportion is set at 5 %. Due to the variability in constituent materials and testing, concrete must be designed to achieve a target mean strength, incorporating a margin above the characteristic strength to ensure a 95 % confidence level in meeting it. This margin is typically set at 1.645 standard deviations. For general concrete production, the standard deviation could be as big as 5 MPa.

Table 5 lists the strength deviation of 28d compressive strength (σ_{sd}), and each σ_{sd} is illustrated in Fig. 21. Firstly, all σ_{sd} values are under 5 MPa, indicating that the batch of cast concrete possesses reliability on compressive results. Secondly, the σ_{sd} of normal concrete under the normal curing condition exhibits a single increasing trend as PSD shifts from upper to lower, rising from 0.49 MPa to 3.34 MPa. A similar trend is also observed in normal concrete treated by lab standard curing, but the range of σ_{sd} narrows

to 0.50 MPa to 1.49 MPa, which means the lab standard curing condition could reduce the disparity degree in compressive strength. In addition, the σ_{sd} of recycled concrete under the lab standard curing condition also shows a single increasing trend, and the σ_{sd} of recycled concrete, under the lab standard curing condition, with PSD of upper and median approximately are equivalent to that of corresponding normal concrete as well as the values are also lower than those of recycled concrete with the same PSD under the normal curing,

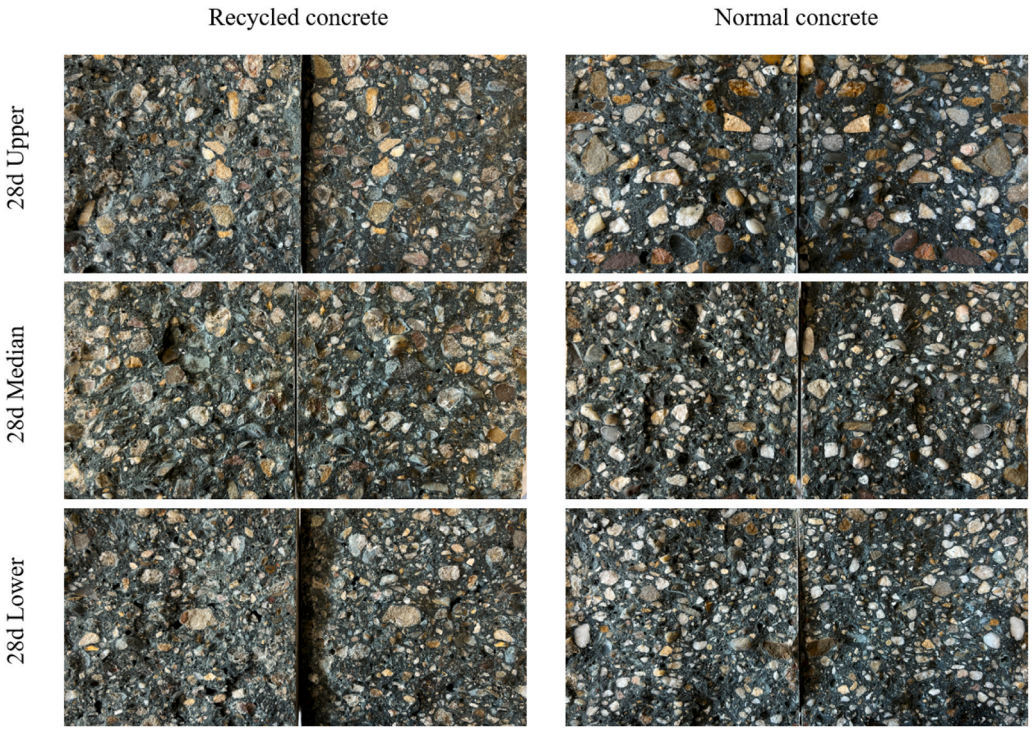

Fig. 20. Failure surface characteristics.

Table 5
Strength deviation of 28d compressive strength (σ_{sd}).

Type	PSD	Normal curing ($f_{cu,28d}$) /MPa			σ_{sd} /MPa	Lab standard curing ($f_{cu,28d}$) /MPa			σ_{sd} /MPa
Recycled concrete	Upper	65.66	61.86	63.20	1.57	62.93	63.04	64.16	0.56
	Median	62.82	67.09	65.05	1.74	66.68	65.16	63.31	1.38
	Lower	64.33	64.93	64.65	0.25	69.15	68.58	61.55	3.46
Normal concrete	Upper	59.21	60.26	60.24	0.49	59.81	60.86	59.79	0.50
	Median	60.90	62.02	65.72	2.06	64.91	63.82	67.28	1.44
	Lower	66.26	68.48	60.54	3.34	68.51	65.21	65.52	1.49

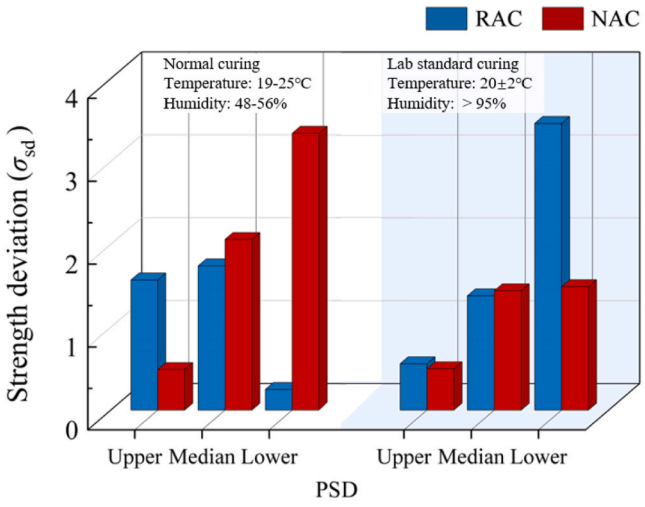

Fig. 21. Strength deviation (σ_{sd}).

respectively. In addition, the σ_{sd} of recycled concrete with lower PSD under the normal curing condition exhibits the minimum value of 0.25 MPa, showing a significant difference compared to recycled concrete with lower PSD under the lab standard curing. The reason needs to be further checked with more concrete specimens. Besides, as only three specimens were tested for each configuration, the statistical conclusions from a small sample size should take reliable issues into account. In spite of this, the maximum coefficient of variation within this dataset is only around 5 %. While the value of the coefficient of variation cannot directly confirm the reliability of the standard deviation under small sample conditions, it indirectly suggests that the data are relatively stable, and the standard deviation may hold certain significance.

4. Conclusion

This study investigated the effects of different particle size distributions (PSD) of high-quality recycled coarse aggregate (HqRCA) and curing conditions on the compressive strength, tensile splitting strength, and strength development of recycled concrete. The experimental results demonstrate that, in terms of compressive strength, using HqRCA as a replacement for preparing natural coarse aggregates (NCA) in concrete preparation is feasible (The 28-day compressive strength is around 64 MPa). Moreover, when HqRCA is used to replace NCA in the same mass to prepare concrete, lower PSD tends to exhibit better compressive performance. Additionally, concrete strength, particularly tensile splitting strength, is significantly influenced by curing conditions. The tensile splitting strength of lab standard-cured normal concrete at 28 days was, on average, 13.26 % higher than that of normal-cured concrete at the same age. For recycled concrete, this increase was 14.39 %. Favourable curing conditions also ensured continued strength development in recycled concrete. Compared to the fracture characteristics of normal concrete under tensile splitting loads, recycled concrete specimens also exhibited fracture planes with many coarse aggregate particles intersecting the fracture surface, rather than predominantly debonding failure modes. This suggests that the bond behaviour between HqRCA and the new cementitious matrix is reliable. Finally, the standard deviations of the 28-day compressive strength of recycled concrete specimens, as a key indicator referenced by industries for controlling concrete production, are all under 5 MPa. While the experimental data, according to the maximum coefficient of variation within this dataset, was only around 5 % and exhibited low variability, the sample size was still limited, which may raise concerns about statistical reliability. Ongoing research should enlarge the sample size to enhance the robustness of the findings.

CRediT authorship contribution statement

Shuai Zong: Writing – original draft, Validation, Investigation, Formal analysis, Data curation, Conceptualization. **Cheng Chang:** Writing – review & editing, Validation, Methodology, Data curation. **Peter Rem:** Writing – review & editing, Supervision, Funding acquisition, Conceptualization. **Abraham T. Gebremariam:** Writing – review & editing, Resources, Conceptualization. **Francesco Di Maio:** Writing – review & editing, Supervision, Funding acquisition. **Yiyan Lu:** Writing – review & editing, Supervision, Funding acquisition.

Declaration of Competing Interest

The authors declare the following financial interests/personal relationships which may be considered as potential competing interests: During the research, Peter Rem was both board member and owner of equity/stock of C2CA Technology. There are no additional issues.

Acknowledgement

This work was supported by the European Union Horizon's 2020 funded Project "Innovative Circular Economy Based solutions demonstrating the Efficient Recovery of valuable material resources from the Generation of representative end-of-life building materials" (ICEBERG, grant agreement No. 869336).

The authors are thankful to Ali Vahidi, Ron Penners, Maarten Bakker, Richard Idzes, and Ton Blom for their support during the experiment preparation and operation. Lastly, thanks to C2CA for their provision of recycled coarse aggregates.

Data availability

The authors do not have permission to share data.

References

[1] J.D. Morley, R.J. Myers, Y. Plancherel, P.R. Brito-Parada, A database for the stocks and flows of sand and gravel, Resources 11 (2022) 72, https://doi.org/10.3390/resources11080072.
[2] Louise Gallagher, Pascal Peduzzi, 2019, , Sand and Sustainability: Finding New Solutions for Environmental Governance of Global Sand Resources.⟨https://espace.library.uq.edu.au/view/UQ:a4ded77⟩(Accessed 5 October 2024).
[3] US EPA, Construction and Demolition Debris: Material-Specific Data, 2023. ⟨https://www.epa.gov/facts-and-figures-about-materials-waste-and-recycling/construction-and-demolition-debris-material⟩ (Accessed 9 September 2024).

[4] Eurostat, Waste statistics, 2020. ⟨https://ec.europa.eu/eurostat/tgm/refreshTableAction.do?tab=table&plugin= 1&pcode=ten00106&language=en⟩ (Accessed 2 April 2020).

[5] S. Zong, Y. Lu, W. Ma, Y. Yan, C. Lin, Behaviour of steel-fibre-reinforced recycled concrete-filled square steel tubular short columns under axial compressive load, Eng. Struct. 271 (2022) 114894, https://doi.org/10.1016/j.engstruct.2022.114894.

[6] P. Land, 2019, The Swiss Example: Using Recycled Concrete,⟨https://global-recycling.info/archives/2956⟩(Accessed 5 May 2024).

[7] Energy Smart Communities Initiative, Samwoh Eco Green Building, 2016. ⟨https://www.esci-ksp.org/archives/project/samwoh-eco-green-building⟩ (Accessed 5 May 2024).

[8] R.V. Silva, J. de Brito, R.K. Dhir, Use of recycled aggregates arising from construction and demolition waste in new construction applications, J. Clean. Prod. 236 (2019) 117629, https://doi.org/10.1016/j.jclepro.2019.117629.

[9] Z. Deng, B. Liu, B. Ye, P. Xiang, Mechanical behavior and constitutive relationship of the three types of recycled coarse aggregate concrete based on standard classification, J. Mater. Cycles Waste Manag. 22 (2020) 30–45, https://doi.org/10.1007/s10163-019-00922-5.

[10] B. Wang, L. Yan, Q. Fu, B. Kasal, A comprehensive review on recycled aggregate and recycled aggregate concrete, Resour. Conserv. Recycl. 171 (2021) 105565, https://doi.org/10.1016/j.resconrec.2021.105565.

[11] Y. Tang, J. Xiao, H. Zhang, Z. Duan, B. Xia, Mechanical properties and uniaxial compressive stress-strain behavior of fully recycled aggregate concrete, Constr. Build. Mater. 323 (2022) 126546, https://doi.org/10.1016/j.conbuildmat.2022.126546.

[12] Y. Wang, H. Zhang, Y. Geng, Q. Wang, S. Zhang, Prediction of the elastic modulus and the splitting tensile strength of concrete incorporating both fine and coarse recycled aggregate, Constr. Build. Mater. 215 (2019) 332–346, https://doi.org/10.1016/j.conbuildmat.2019.04.212.

[13] S. Zong, Z. Liu, S. Li, Y. Lu, A. Zheng, Stress-strain behaviour of steel-fibre-reinforced recycled aggregate concrete under axial tension, J. Clean. Prod. 278 (2021) 123248, https://doi.org/10.1016/j.jclepro.2020.123248.

[14] S. Arora, S.P. Singh, Analysis of flexural fatigue failure of concrete made with 100% Coarse Recycled Concrete Aggregates, Constr. Build. Mater. 102 (2016) 782–791, https://doi.org/10.1016/j.conbuildmat.2015.10.098.

[15] S.I. Mohammed, K.B. Najim, Mechanical strength, flexural behavior and fracture energy of Recycled Concrete Aggregate self-compacting concrete, Structures 23 (2020) 34–43, https://doi.org/10.1016/j.istruc.2019.09.010.

[16] H. Guo, C. Shi, X. Guan, J. Zhu, Y. Ding, T.-C. Ling, H. Zhang, Y. Wang, Durability of recycled aggregate concrete – a review, Cem. Concr. Compos. 89 (2018) 251–259, https://doi.org/10.1016/j.cemconcomp.2018.03.008.

[17] S. Silva, L. Evangelista, J. de Brito, Durability and shrinkage performance of concrete made with coarse multi-recycled concrete aggregates, Constr. Build. Mater. 272 (2021) 121645, https://doi.org/10.1016/j.conbuildmat.2020.121645.

[18] J. Xiao, W. Li, Z. Sun, D.A. Lange, S.P. Shah, Properties of interfacial transition zones in recycled aggregate concrete tested by nanoindentation, Cem. Concr. Compos. 37 (2013) 276–292, https://doi.org/10.1016/j.cemconcomp.2013.01.006.

[19] D. Pedro, J. de Brito, L. Evangelista, Durability performance of high-performance concrete made with recycled aggregates, fly ash and densified silica fume, Cem. Concr. Compos. 93 (2018) 63–74, https://doi.org/10.1016/j.cemconcomp.2018.07.002.

[20] C. Liang, B. Pan, Z. Ma, Z. He, Z. Duan, Utilization of CO2 curing to enhance the properties of recycled aggregate and prepared concrete: a review, Cem. Concr. Compos. 105 (2020) 103446, https://doi.org/10.1016/j.cemconcomp.2019.103446.

[21] R. Wang, N. Yu, Y. Li, Methods for improving the microstructure of recycled concrete aggregate: a review, Constr. Build. Mater. 242 (2020) 118164, https://doi.org/10.1016/j.conbuildmat.2020.118164.

[22] M. Florea, Z. Ning, H. Brouwers, Smart crushing of concrete and activation of liberated concrete fines, University of Eindhoven, Department of the Built Environment, Unit Building Physics and Services: Eindhoven, The Netherlands, 2012.

[23] Y. Menard, K. Bru, S. Touze, A. Lemoign, J.E. Poirier, G. Ruffie, F. Bonnaudin, F. Von Der Weid, Innovative process routes for a high-quality concrete recycling, Waste Manag. 33 (2013) 1561–1565, https://doi.org/10.1016/j.wasman.2013.02.006.

[24] M. Shigeishi, Separation and collection of coarse aggregate from waste concrete by electric pulsed power, AIP Conf. Proc. 1887 (2017) 020077, https://doi.org/10.1063/1.5003560.

[25] A.T. Gebremariam, F. Di Maio, A. Vahidi, P. Rem, Innovative technologies for recycling End-of-Life concrete waste in the built environment, Resour. Conserv. Recycl. 163 (2020) 104911, https://doi.org/10.1016/j.resconrec.2020.104911.

[26] A. Vahidi, A.T. Gebremariam, F. Di Maio, K. Meister, T. Koulaeian, P. Rem, RFID-based material passport system in a recycled concrete circular chain, J. Clean. Prod. 442 (2024) 140973, https://doi.org/10.1016/j.jclepro.2024.140973.

[27] C. Chang, F.D. Maio, P. Rem, A.T. Gebremariam, F. Mehari, H. Xia, Cluster-based identification algorithm for in-line recycled concrete aggregates characterization using Laser-Induced Breakdown Spectroscopy (LIBS), Resour. Conserv. Recycl. 185 (2022) 106507, https://doi.org/10.1016/j.resconrec.2022.106507.

[28] C. Chang, F. Di Maio, R. Bheemireddy, P. Posthoorn, A.T. Gebremariam, P. Rem, Rapid quality control for recycled coarse aggregates (RCA) streams: multi-sensor integration for advanced contaminant detection, Comput. Ind. 164 (2025) 104196, https://doi.org/10.1016/j.compind.2024.104196.

[29] BS EN, Aggregates for concrete (BS EN 12620:2013), 2013.

[30] E. Özbay, M. Erdemir, H.İ. Durmuş, Utilization and efficiency of ground granulated blast furnace slag on concrete properties – a review, Constr. Build. Mater. 105 (2016) 423–434, https://doi.org/10.1016/j.conbuildmat.2015.12.153.

[31] W. Matthes, A. Vollpracht, Y. Villagrán, S. Kamali-Bernard, D. Hooton, E. Gruyaert, M. Soutsos, N. De Belie, Ground granulated blast-furnace slag, in: Properties of Fresh and Hardened Concrete Containing Supplementary Cementitious Materials, Springer, Cham, 2018, pp. 1–53, https://doi.org/10.1007/978-3-319-70606-1_1.

[32] H. Zhang, X. Xu, W. Liu, B. Zhao, Q. Wang, Influence of the moisture states of aggregate recycled from waste concrete on the performance of the prepared recycled aggregate concrete (RAC) – a review, Constr. Build. Mater. 326 (2022) 126891, https://doi.org/10.1016/j.conbuildmat.2022.126891.

[33] C. Thomas, J. Setién, J.A. Polanco, J. de Brito, F. Fiol, Micro- and macro-porosity of dry- and saturated-state recycled aggregate concrete, J. Clean. Prod. 211 (2019) 932–940, https://doi.org/10.1016/j.jclepro.2018.11.243.

[34] C.S. Poon, Z.H. Shui, L. Lam, H. Fok, S.C. Kou, Influence of moisture states of natural and recycled aggregates on the slump and compressive strength of concrete, Cem. Concr. Res. 34 (2004) 31–36, https://doi.org/10.1016/S0008-8846(03)00186-8.

[35] K.P. Verian, W. Ashraf, Y. Cao, Properties of recycled concrete aggregate and their influence in new concrete production, Resour. Conserv. Recycl. 133 (2018) 30–49, https://doi.org/10.1016/j.resconrec.2018.02.005.

[36] BS EN, Testing hardened concrete. Compressive strength of test specimens (BS EN 12390–6:2019), 2019.

[37] BS EN, Testing hardened concrete. Tensile splitting strength of test specimens (BS EN 12390–6:2023), 2023.

[38] X. Ke, Z. Chen, J. Xue, Y. Su, Experimental study on the bearing capacity of recycled aggregate concrete-filled square steel tube short columns under axial compression, Eng. Mech. 30 (2013) 35–41, https://doi.org/10.6052/j.issn.1000-4750.2011.11.0759.

[39] M.S. Meddah, S. Zitouni, S. Belâabes, Effect of content and particle size distribution of coarse aggregate on the compressive strength of concrete, Constr. Build. Mater. 24 (2010) 505–512, https://doi.org/10.1016/j.conbuildmat.2009.10.009.

[40] P.K. Mehta, P.J.M. Monteiro, Microstructure of concrete, in: Concrete: Microstructure, Properties, and Materials, 4th Edition, McGraw-Hill Education, New York, 2014. ⟨https://www.accessengineeringlibrary.com/content/book/9780071797870/chapter/chapter2⟩ (Accessed 31 December 2024).

[41] Y. Tu, H. Yu, H. Ma, W. Han, Y. Diao, Experimental study of the relationship between bond strength of aggregates interface and microhardness of ITZ in concrete, Constr. Build. Mater. 352 (2022) 128990, https://doi.org/10.1016/j.conbuildmat.2022.128990.

[42] J. Montero, S. Laserna, Influence of effective mixing water in recycled concrete, Constr. Build. Mater. 132 (2017) 343–352, https://doi.org/10.1016/j.conbuildmat.2016.12.006.

[43] Y. Gao, G. De Schutter, G. Ye, Z. Tan, K. Wu, The ITZ microstructure, thickness and porosity in blended cementitious composite: effects of curing age, water to binder ratio and aggregate content, Compos. Part B: Eng. 60 (2014) 1–13, https://doi.org/10.1016/j.compositesb.2013.12.021.

[44] Y. Gao, H. Sun, Influence of initial defects on crack propagation of concrete under uniaxial compression, Constr. Build. Mater. 277 (2021) 122361, https://doi.org/10.1016/j.conbuildmat.2021.122361.

[45] W. Cui, M. Liu, H. Song, W. Guan, H. Yan, Influence of initial defects on deformation and failure of concrete under uniaxial compression, Eng. Fract. Mech. 234 (2020) 107106, https://doi.org/10.1016/j.engfracmech.2020.107106.

[46] S.-C. Kou, C.-S. Poon, M. Etxeberria, Influence of recycled aggregates on long term mechanical properties and pore size distribution of concrete, Cem. Concr. Compos. 33 (2011) 286–291, https://doi.org/10.1016/j.cemconcomp.2010.10.003.

[47] EN, Eurocode 2: Design of concrete structures - Part 1–1: General rules and rules for buildings (EN 1992–1-1:2004), 2004.

[48] International Federation for Structure Concrete (fib), fib Model Code for Concrete Structures 2010, 2010.

[49] D.U. Min, J.I.N. Liu, L.I. Dong, D.U. Xiu-li, Mesoscopic simulation study of the influence of aggregate size on mechanical properties and specimen size effect of concrete subjucted to splitting tensile loading, gclx 34 (2017) 54–63, https://doi.org/10.6052/j.issn.1000-4750.2016.02.0122.

[50] Z. Wu, J. Zhang, H. Yu, Q. Wu, B. Da, Computer-aided investigation of the tensile behavior of concrete: relationship between direct and splitting tensile strength, Structures 55 (2023) 453–467, https://doi.org/10.1016/j.istruc.2023.06.019.